Bulgarian Society for NDT
International Journal "NDT Days"
Volume V, Issue 5, Year 2022
ISSN: 2603-4018
eISSN: 2603-4646

Algorithm for Precision Determination of Amplitudes and Phases of Poly-harmonic Signals Harmonic Components in Eddy Current Non-destructive Testing

Victor BAZHENOV, Yuriy KALENYCHENKO, Aleksandr KALENYCHENKO, Sergiy RATSEBARSKIY

National Technical University of Ukraine "Igor Sikorsky Kyiv Polytechnic Institute",
Kyiv, Ukraine,
e-mail: vgbazhenov@gmail.com

Abstract
The development of electronic systems in recent years has made 14-bit field-programmable gate array (FPGA), digital-to-analog converters (DAC) and analog-to-digital converters (ADC) available for mass commercial operation. This created the conditions for the development and application of software and hardware implemented on FPGA algorithms for fast processing of digital signals. Such solutions, in turn, have opened up new opportunities for the proliferation of multi-frequency eddy current systems (MFEC) of non-destructive testing (NDT) in the form of simultaneous processing of different frequencies digital signals, which allows MFEC to compete effectively with pulsed eddy current systems (PEC). In this paper, we present a new algorithm for precise digital measurement of the MFEC amplitude and phase of poly-harmonic signals harmonic components, which is implemented in hardware and software on a 14-bit FPGA. The measurement of the harmonic components amplitude and phase is based on the method of digital signals orthogonal processing, to increase the accuracy of which we prove the need to fulfill the condition of multiplicity of the sample sequence to the size of the digital signal period. Compliance with this condition is achieved by adjusting the length of the sample sequence, which in the proposed algorithm is performed before orthogonal processing. The effect of inaccuracy in establishing the sample sequence length on the measurement errors size in determining the amplitude and phase of the signal harmonic components is simulated using a Monte Carlo simulation. As a result of modeling, it was found that if the multiplicity condition is met, the measurement error is reduced by five orders of magnitude, which indicates the high efficiency of our algorithm. Achieved precision accuracy of measuring the harmonic components amplitude and phase of poly-harmonic signals due to the specified hardware and software implementation of the algorithm allows to create inexpensive, compact, scalable automated digital control systems, measurement data of which can be used to determine individual characteristics of the control object, and for the reconstruction of three-dimensional images, ie in tomographic systems.

Keywords: Algorithm, Phase Measurement, Orthogonal Method, Measurement Error, Non-Destructive Testing, Eddy Current, Multifrequency Signal, Poly-harmonic Signal, Harmonics

1. Introduction

An important condition for the automation of eddy current (EC) NDT operations is a reliable interpretation of the scan results of the objects under control, which is achieved by controlling the excitation signals parameters, such as amplitude and frequency. The latter is one of the most important parameters, because it depends on the depth of penetration of the electromagnetic field into the object under control material, the so-called "skin effect", which is used to characterize surface and subsurface defects, and in some cases microstructures. PEC method of NDT is the most widespread due to the wide range of pulse signal frequencies, which is controlled by applying a pulse shape, and the test result is usually obtained by processing data by Fourier transform or similar in the frequency/time domain, followed by intelligent interpretation.

An alternative to PEC method are MFEC methods of NDT, when the scanning of the object is monitored by certain algorithms signals of specially selected frequency values [1], [2],

[3] or poly-harmonic signals [4], [5], [6]. MFEC have not become as widespread as PEC, due to the complexity of simultaneous supply of frequencies spectrum to the channel, but recently their efficiency has improved due to the introduction of digital processing, including signals synthesis [1], [7], [8]. Thus, the use of modern systems based on FPGA provides automatic simultaneous multi-channel processing of different frequencies signals in the selected range with a given step, which allows to reconstruct defect images on maps of scan results [1], or increase the speed of parallel processing of multifrequency signals while maintaining a high signal-to-noise ratio [9]. For the classification of suitable/unsuitable, the use of an artificial neural network with a radial basis function, which was used to process impedances at five frequencies, was demonstrated [2]. The new approach, based on the use of EC giant magneto-resistive sensor data conversion algorithms and multidimensional optimization procedure, allows to attenuate the signs of artifacts of MFEC and to strengthen the signs of information about defects [3]. At certain values of the excitation signal frequencies, the sensor inductance is almost independent of the lift-off effect, and for the automated selection of such frequencies, algorithms of inverse solvers have been proposed [10]. Also, the connection of MFEC frequencies with the real component of the coil inductance allows to map the weld zones, and as a result to determine the microstructures of these zones with high sensitivity [11], [12]. Simultaneous use of four frequencies and automation of sensor motion provides fast scanning of surface damage of aircraft honeycomb panels with a quality that exceeds optical 3-dimensional scanning [13]. Multifrequency signals in the range of $1 \div 1000kHz$ are used to determine the microstructure of steel rails, namely the depth of steel decarburization as a result of heat treatment [14]. In general, with the use of automated methods and algorithms for pattern recognition, the efficiency of MFEC systems is not inferior to PEC systems, which brings them to the level of tomographic systems [15]. However, the traditional key elements of automation are the intelligent processing of complex algorithms of signal amplitude measured values. Thus, the use of phase characteristics of poly-harmonic and multifrequency signals in EC NDT was limited or impossible.

The improvement of MFEC methods expands their capabilities not only in the parameterization of defects, but also in determining changes in the structure of materials. The study of physical phenomena in solid state physics, in electromagnetic theory, has led to the discovery of new, more informative features in the use of EC methods, which are related to the structure of the studied materials. For example, if, as mentioned above, in MFEC they determine only the amplitudes values of certain frequencies, then we propose in addition to the amplitudes to determine the phase characteristics of higher harmonics, the values of which, as shown by experimental results, are more informative. Traditionally, the procedure of selection of higher harmonics is not simple, requires the use of filters, in addition, for simultaneous measurement requires a park of vector voltmeters or special phase meters, and to build a family of graphs with such primary results, the control time of one component can be measured in hours. Thus, the use of phase characteristics of poly-harmonic and multifrequency signals in eddy current non-destructive testing was limited or impossible.

To overcome the above MFEC limitations, we have proposed a new algorithm for precise digital measurement of the amplitude and phase of the poly-harmonic signal harmonic components. This algorithm is hardware-software implemented on the FPGA and is based on the features of the synthesis of the MFEC excitation signal and orthogonal processing response signals, which are discussed below.

2. Method

To determine the amplitude and phase of the analog response signal harmonic components, which are measured from the output of the EC probe, we used the orthogonal

method of their processing [16], [17]. The method is based on multiplication of presented in the form of sequences of samples of the finite length of the digital response signal, formed by analog-to-digital transformations of response signal, by specially generated digital harmonious orthogonal signals, which are sequences of samples with known amplitude and phase, the frequency of which is equal to the frequency of the harmonic under study, and their length coincides with the length of the digital response signal:

$$\begin{aligned} s_{cos_k}(x) &= DRS(x) * DHOS_{sin}(x), \\ s_{sin_k}(x) &= DRS(x) * DHOS_{cos}(x), \end{aligned} \tag{1}$$

where k is the harmonic number, $s_{cos_k}(x), s_{sin_k}(x)$ are intermediate signals, $DRS(x)$ is digital response signal, $DHOS_{cos}(x), DHOS_{sin}(x)$ are digital harmonious orthogonal signals, x is the sample number in the sequence, $0 \le x < M, x = 0,1,2,3,4$ ..., and M is its length, f is the excitation signal frequency at the input of the EC converter, obtained by digital-to-analog conversion of a discrete digital signal generated by direct digital synthesis (DDS). The main principle is that we use for the first time a clock signal from the same source for synthesis of the excitation signal and for sampling of the response signal.

It is well known that:

$$\begin{aligned} &\sin(\omega_1 t + \varphi_1) * \sin(\omega_2 t + \varphi_2) = \\ &= \frac{1}{2}\cos\big((\omega_1 - \omega_2)t + \varphi_1 - \varphi_2\big) - \frac{1}{2}\cos\big((\omega_1 + \omega_2)t + \varphi_1 + \varphi_2\big), \\ &\sin(\omega_1 t + \varphi_1) * \cos(\omega_2 t + \varphi_2) = \\ &= \frac{1}{2}\sin\big((\omega_1 - \omega_2)t + \varphi_1 - \varphi_2\big) + \frac{1}{2}\sin\big((\omega_1 + \omega_2)t + \varphi_1 + \varphi_2\big), \end{aligned} \tag{2}$$

where respectively, when $\omega = \omega_1 = \omega_2$ and $\varphi_2 = 0$:

$$\begin{aligned} \sin(\omega t + \varphi) * \sin(\omega t) &= \frac{1}{2}\cos(\varphi) - \frac{1}{2}\cos(\omega t + \varphi), \\ \sin(\omega t + \varphi) * \cos(\omega t) &= \frac{1}{2}\cos(\varphi) + \frac{1}{2}\sin(\omega t + \varphi). \end{aligned} \tag{3}$$

From expression (3) it follows that after multiplying two signals of the same frequency, the result will have a constant component $\frac{1}{2}\cos(\varphi)$ or $\frac{1}{2}\sin(\varphi)$ and a variable harmonic component $\frac{1}{2}\cos(2\omega t + \varphi)$ or $\frac{1}{2}\sin(2\omega t + \varphi)$. A sine wave is a harmonic signal, the properties signal of which:

$$\begin{aligned} \int \sin(\omega t)dt &= \int_0^{N_0 T} \sin(\omega t)dt = 0 \\ \int \cos(\omega t)dt &= \int_0^{N_0 T} \cos(\omega t)dt = 0 \end{aligned} \tag{4}$$

where T is the signal period, $N_0 = 1,2,3,4$ ... ($N_0 \in \mathbb{Z}^+$) is the number of its periods. Thus, the integration of the results of signal multiplication, which are intermediate signals $s_{cos_k}(x), s_{sin_k}(x)$ in expression (1), depends only on the constant component, because the integration of all harmonic components according to (4) is equal to zero in the case of compliance with the condition that the number of periods N_0 belongs to the set of positive integer $\mathbb{Z}^+$. Failure to comply with this condition leads to an error in determining the phase and amplitude of the harmonic components, the size of which is investigated below by simulation.

Given that we operate with digital signals, instead of analog integration we will use numerical integration, also known as the average value, of expression (1), which will look as follows:

$$\begin{gathered}\frac{1}{M_{IS}}\sum_{x=0}^{M_{IS}-1} s_{cos_k}(x) = \frac{1}{2}A_k\cos(\varphi_k),\\ \frac{1}{M_{IS}}\sum_{x=0}^{M_{IS}-1} s_{sin_k}(x) = \frac{1}{2}A_k\sin(\varphi_k),\\ M_{IS} = N\cdot n\end{gathered} \tag{5}$$

where M_{IS} is the length of the sequence of the intermediate signal, and N is the number of its periods with a fractional part, or $N \in \mathbb{R}^+$, $n = \frac{f_{sr}}{f}$ is the number of points in the period of the intermediate signal, where f_{sr} is the clock signal frequency (CS), f is the excitation signal frequency , A_k is amplitude of the k-th harmonic and φ_k is phase of the k-th harmonic of the digital response signal.

From expressions (5), using the function of the two-argument arctangent, we obtain the value of the phase of the k-th harmonic of the digital response signal:

$$\varphi_k = \operatorname{atan2}\left(\frac{\frac{1}{M_{IS}}\sum_{x=0}^{M_{IS}-1} s_{cos_k}(x)}{\frac{1}{M_{IS}}\sum_{x=0}^{M_{IS}-1} s_{sin_k}(x)}\right) = \operatorname{atan2}\left(\frac{\frac{1}{M_{IS}}\sum_{x=0}^{M_{IS}-1} DRS(x) * \mathrm{DHOS}(x)}{\frac{1}{M_{IS}}\sum_{x=0}^{M_{IS}-1} DRS(x) * \mathrm{DHOS}(x)}\right) \tag{6}$$

Similarly, we obtain the value of the amplitude of the k-th harmonic of the digital response signal:

$$\begin{gathered}A_k = 2\sqrt{(\frac{1}{M_{IS}}\sum_{x=0}^{M_{IS}-1} s_{cos_k}(x))^2 + (\frac{1}{M}\sum_{x=0}^{M_{IS}-1} s_{sin_k}(x))^2} =\\ = 2\sqrt{(\frac{1}{M_{IS}}\sum_{x=0}^{M_{IS}-1} DRS(x) * DHOS(x))^2 + (\frac{1}{M}\sum_{x=0}^{M_{IS}-1} DRS(x) * \mathrm{DHOS}(x))^2}\end{gathered} \tag{7}$$

Obviously, to comply with the condition of the signal number of periods N_0 to the set of positive integer $\mathbb{Z}^+$, the sequence length of the intermediate signal M_{IS} must be a multiple of the digital response signal period T_{DRS}, which can be achieved by algorithmically setting the sequence length M_{IS} of the intermediate signal.

3. Modelling

To assess the effect of inaccuracy in establishing the length of the sequence M_{IS} on the size of errors in determining the amplitude and phase of harmonic components, we investigated the relationship between the fractional part of the number of periods N in the digital response signal, which is called the incompleteness of the integration interval, and the mean absolute error of the amplitude and phase.

The simulation was performed using a Monte Carlo simulation in the MATLAB software package [18]. Simulation characteristics: 25 thousand cycles, step 1% of the integration interval

incompleteness, whole periods 39. Simulations with 1, 5, 10 thousand cycles and steps 0.5%, 2%, 5% of the integration interval incompleteness at the whole number of 8 and 15 periods were also performed.

To artificially introduce the incompleteness of the integration interval during the simulation, formulas (5) were changed as follows:

$$\frac{1}{2}A_k \cos(\varphi_k) = \frac{1}{M_0 + j} \sum_{x=0}^{M_0+j-1} DRS(x) * DHOS(x), \quad (8)$$

where M_0 is the length of the sequence of the intermediate signal, a multiple of the digital response signal period length, j is the number of excess M_{IS} sequence points to M_0.

Formula (8) shows the method of obtaining one of the intermediate results of the calculation, the average value of the sequence used to calculate the values of the selected harmonic amplitude and phase. Fig. 1 presents the results of modeling the dependence of the mean absolute error on the incompleteness of the integration interval for odd harmonics up to and including the ninth. Here, the X axis is the value of $\frac{jf}{f_{sr}}$, or the incompleteness of the integration interval, and the Y axis is the modulus of the mean absolute error in volts for the amplitude $|\Delta A|$ and in degrees for the phase $|\Delta\varphi|$. It is observed that for all harmonics the error in amplitude and phase is minimal at points 0 and 1, according to the simulation results it is less than the error of the uncontrolled signal by 5 orders of magnitude. As the number of harmonics k increases, the chaotic error increases in amplitude and phase, while the absolute size of the error in amplitude almost does not change, and in phase increases significantly.

3. Algorithm

To comply with the condition of the integer number of periods, we have proposed the following algorithm, which is implemented as follows (Fig. 2). First, the excitation signal frequency is selected so that it is defined as the clock signal frequency divided by the positive integer n_0 (the nearest less positive integer than n), if it does not correspond to the set frequency. Then the number of periods N in the sequence of length M_{IS} is adjusted, which should be determined by a positive integer N_0 (the nearest less positive integer than N), and accordingly, the length of the sequence M_{IS} is reduced to $M_0 = N_0 \cdot n_0$. When the condition regarding the integer number of periods is met, the values of the amplitude and phase of the harmonic components are calculated.

Response signal sampling is provided using 14-bit ADCs with the maximum sampling rate of 125 MHz. This sampling rate can be changed by frequency divider by 2^i. The period is generated using a 14-bit DAC. It is known that the output signal frequency is determined according to the expression:

$$f = \frac{f_{sr}}{n}, \quad (9)$$

and above it was shown that to reduce the error in determining the amplitude and phase, the value of n must belong to the set of positive integer $\mathbb{Z}^+$. Accordingly, if a certain excitation signal frequency is set, the initial operating conditions of the DAC must be taken into account.

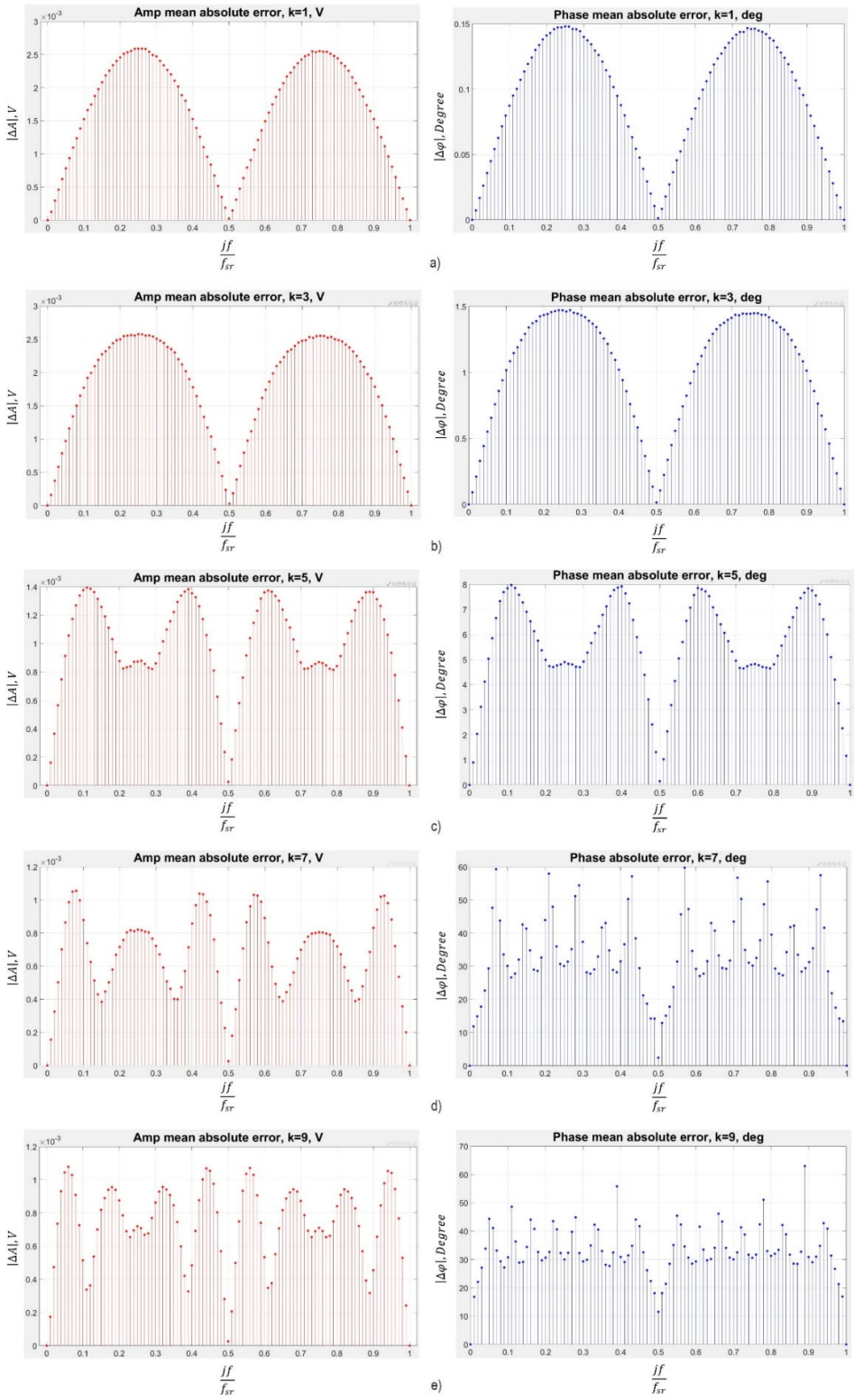

Fig. 1. Dependence of the mean absolute error on the incompleteness of the integration interval: a) harmonic $k = 1$, amplitude and phase, b) harmonic $k = 3$, amplitude and phase, c) harmonic $k = 5$, amplitude and phase, d) harmonic $k = 7$, amplitude and phase, e) harmonic $k = 9$, amplitude and phase

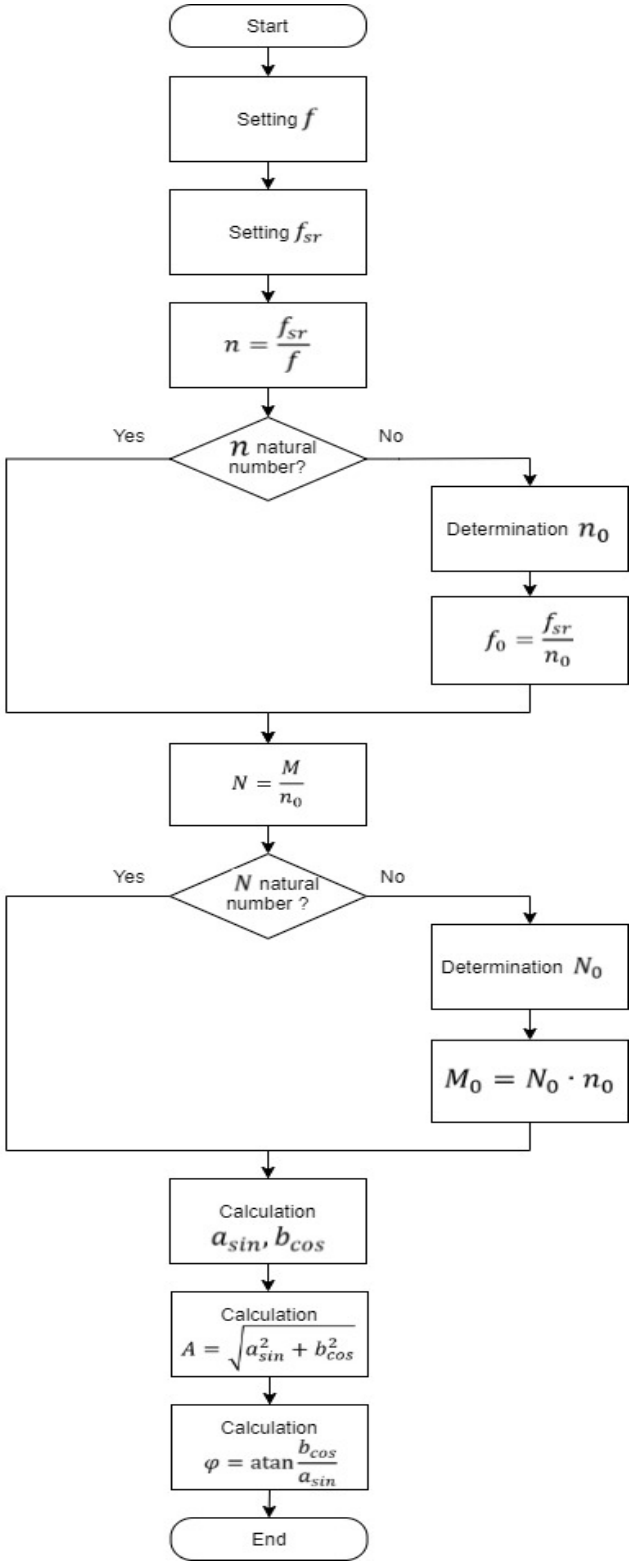

Fig. 2. Algorithm for precise determination of amplitude and phase.

To do this, the calculation is performed $n = \frac{f_{sr}}{f}$, and if the result is fractional, it is rounded to the smallest modulo, with a slight change in the excitation signal frequency. For example, if the

excitation signal frequency is set as 40,000 Hz, its actual frequency will be 40,064.10 Hz, which in no way affects the results of the EC inspection, for which the step of changing the frequency is at least 1000 Hz.

4. Conclusions

The use of the proposed algorithm has reduced the errors in determining the amplitudes and phases of the harmonics of the response signals during their processing by the orthogonal method by five orders of magnitude. The disadvantage of this algorithm is the slight difference between the specified and actually used frequencies of the excitation signal, but as shown above in the example, the effect of this difference can be neglected.

The developed algorithm can be integrated into any digital system using orthogonal signal processing methods. For example, we have developed and manufactured a compact digital computer-integrated automated control system that allows to determine the amplitude-phase-amplitude characteristics of the harmonic components of poly-harmonic signals and obtain the final result in the form of a graphs family or maps of reconstructed images from the scanned plane without the use of a measuring instruments fleet. Data received in amplitude-phase-amplitude characteristics measurements can be further processed by means of intellectual methods.

References

1. J. R. S. Avila, Z. Chen, H. Xu and W. Yin. A multi-frequency NDT system for imaging and detection of cracks, 2018 IEEE International Symposium on Circuits and Systems (ISCAS), 2018, pp. 1-4.
2. Martínez-Martínez, V.; Garcia-Martin, J.; Gomez-Gil, J. RBF-Neural Network Applied to the Quality Classification of Tempered 100Cr6 Steel Cams by the Multi-Frequency Nondestructive Eddy Current Testing, Metals, Volume 7, 2017, p. 385.
3. Oleksii Karpenko, Anton Efremov, Chaofeng Ye, Lalita Udpa. Multi-frequency fusion algorithm for detection of defects under fasteners with EC-GMR probe data. NDT & E International, Volume 110, 2020, p. 102227.
4. Svatoš J., Pospíšil T., Vedral J. Application of poly-harmonic signals to eddy-current metal detectors and to advanced classification of metals, Metrol, Meas. Syst, vol. 25, no. 2, 2018, pp. 387–402.
5. Svatoš, J. Single-tone and Polyharmonic Eddy Current Metal Detection and Non-Destructive Testing Education Software. J. Phys.: Conf. Ser., Volume 772, 2016, p. 012052.
6. Yu. Kalenychenko, V. Bazhenov, A. Kalenychenko, V. Kjval, S. Ratsebarskiy. Determination of Mechanical Properties of Paramagnetic Materials by Multi-frequency Method. International Journal “NDT Days”, Volume II, Issue 4, 2019, pp. 406-416.
7. Y. Kuts, A. Protasov, I. Lysenko, O. Dugin, O. Bliznuk and V. Uchanin. Using multidifferential transducer for pulsed eddy current object inspection. 2017 IEEE First Ukraine Conference on Electrical and Computer Engineering (UKRCON), 2017, pp. 826-829.
8. V. Bazhenov, A. Protasov and K. Gloinik. Increasing of operation speed of digital eddy current defectoscopes based on frequency synthesizer. 2017 IEEE Microwaves, Radar and Remote Sensing Symposium (MRRS), 2017, pp. 155-158.
9. Ziqi Chen, Jorge R. Salas-Avlia, Yang Tao, Wuliang Yin, Qian Zhao, and Zhijie Zhang. A novel hybrid serial/parallel multi-frequency measurement method for impedance analysis in eddy current testing. Review of Scientific Instruments, Volume 91, 2020, p. 024703.
10. Mingyang Lu, Xiaobai Meng, Ruochen Huang, Liming Chen, Anthony Peyton, Wuliang Yin. Lift-off invariant inductance of steels in multi-frequency eddy-current testing. NDT & E International, Volume 121, 2021, p. 102458.
11. Xu, Hanyang; Lu, Mingyang; Avila, J R Salas; Zhao, Qian; Zhou, F; Meng, Xiaobai; Yin, Wuliang. Imaging a weld cross-section using a novel frequency feature in multi-frequency eddy

current testing. Non-Destructive Testing and Condition Monitoring, Volume 61, 2019, pp. 738-743(6).
12. Z. Zhou, M. Qin, Y. Xie, J. Tan and H. Bao. Experimental Study of Microstructures in Bias Weld of Coiled Tubing Steel Strip With Multi-Frequency Eddy Current Testing. IEEE Access, Volume 8, 2020, pp. 48241-48251.
13. Reyno, Tyler and Underhill, P. Ross and Krause, Thomas W. and Marsden, Catharine and Wowk, Diane. Surface Profiling and Core Evaluation of Aluminum Honeycomb Sandwich Aircraft Panels Using Multi-Frequency Eddy Current Testing. Sensors, 17(9), 2017, p. 2114.
14. W. Zhu, W. Yin, S. Dewey, P. Hunt, C.L. Davis, A.J. Peyton. Modeling and experimental study of a multi-frequency electromagnetic sensor system for rail decarburisation measurement. NDT & E International, Volume 86, 2017, pp. 1-6.
15. Dingley, Gavin and Soleimani, Manuchehr, 2021. Multi-Frequency Magnetic Induction Tomography System and Algorithm for Imaging Metallic Objects. Sensors, 21(11), p. 3671.
16. Dorofeev, A. L.; Kazamanov, Iu. G.. *Electromagnetic defectoscopy.* Moscow: Mashinostroenie, 1980.
17. H. Bohdan, V. Bazhenov and A. Protasov. Development of a discrete orthogonal method for determining the phase shift between high-frequency radio impulse signals. IEEE Microwaves, Radar and Remote Sensing Symposium (MRRS), 2017, pp. 191-194.
18. Nicolas Chopin, Omiros Papaspiliopoulos. An Introduction to Sequential Monte Carlo. Springer, 2020, p. 402.